Controlled Surface Texturing of Dental Implants via Q-Switched Nd:YAG Laser: Toward Enhanced Osseointegration

Jin-Woo KIM *, Young-Tae YOU

Department of Mechanical Engineering, Chosun University, 303, Pilmun-daero, Dong-gu, Gwangju 61452, Korea

http://doi.org/10.5755/j02.ms.40897

Received 20 March 2025; accepted 30 May 2025

This study aims to propose an ideal surface treatment method that overcomes the disadvantages of the existing implant surface treatment method and increases the surface area per unit area of the implant for enhanced adhesion between the implant and bone tissue. Generally used implants do not have a screw structure or surface treatment method according to the bone quality of the human body. It is essential to establish precise and systematic process parameters when performing the surface treatment of implants using lasers. Therefore, this study intends to use a Q-switching Nd:YAG laser with a wavelength of 1.06 um to develop a process for modifying the surface of an implant so that it can become a biocompatible structure. In this study, the processing characteristics of a pulsed laser are examined by analyzing the effects of laser beam overlap, variations in laser power, and increases in duty cycle on the resulting scribing width. The results of this study suggest that implant surface treatment technology using lasers will be secured and used for actual implant surface treatment.

Keywords: Nd:YAG laser, step size, implant, surface processing, titanium.

1. INTRODUCTION

In recent decades, the worldwide demand for implants has continued to increase at an alarming rate. Wide range of biomaterials have been used and are being developed for orthopaedic implants, including metallic, ceramic, and polymeric materials. Metallic biomaterials have the advantages of high strength and toughness, easy processing, and good biocompatibility [1, 2].

Among the clinically applied metallic biomaterials, titanium (Ti) and its alloys, such as Ti6Al4V, are the most popular candidates for bone implants due to their excellent mechanical properties (high mechanical strength, low density, immunity to corrosion) and superior biocompatibility, compared to conventional materials such as stainless steel 316L and cobalt–chromium (CoCr) alloys [3].

Dental implant surface modification is a critical area of research aimed at enhancing the osseointegration and longevity of dental implants [4 – 10].

In the preliminary study, the energy density per pulse, heat input, and metallurgical aspects were analyzed according to the focus position of the laser beam, pulse irradiation time of the laser beam, and pulse repetition rate [11]. Based on our experience performing various analyses using lasers, we would like to present a new process to give titanium good surface properties.

This study aims to propose an ideal surface treatment method that overcomes the disadvantages of the existing implant surface treatment method and increases the surface area per unit area of the implant for enhanced adhesion between the implant and bone tissue. Generally used implants do not have a screw structure or surface treatment method according to the bone quality of the human body.

Previous studies on surface modification of implants using laser are as follows. The surface area of the implant was improved by irradiating the aluminum oxide powder-blasted implant with a laser beam between the screw blade and the bone to form a surface hole of 30 to 50 mm in size. Furthermore, the size and shape of the secondary structure resulting from the melting processes were studied, and EDS analysis was performed to analyze the chemical properties of the titanium surface [12]. The ablated surface layer was studied by irradiating the implant surface by changing the pulse duration (30 ns) and pulse energy (0.5 – 5 J) of the Nd:glass laser [13, 14].

The machined implant and the machined and laser surface-treated implant were attached to the rabbit tibia, and then forcefully removed (removal torque) to compare and evaluate whether the contact interface between the bone and the implant was well bonded [15].

In tests made with the short pulse Cr-F UV laser on the Ti-6Al-4V and Ti-6.8Mo-4.5Fe-1.5Al alloys [16 – 18] the relatively smooth, crack-free nanocrystalline surface layers were obtained containing significant amounts of martensite.

Since the oxide film formation is not stable during implant surface treatment by the existing commercial Nd:YAG laser, the morphological aspects, and chemical properties were studied after polishing and structurally changing the surface of the round bar for implant material using UV-type ArF and KrF excimer lasers [19]. However, it was not efficient in terms of productivity, as additional equipment was required to implement vacuum conditions and continuous beam irradiation was performed to improve the surface area. The change in the surface morphology of the central part of the irradiated area was investigated by changing the laser wavelength on the surface of titanium, an implant material. In addition, the surface morphological

* Corresponding author: J. Kim
E-mail address: *jinu763@chosun.ac.kr*

characteristics of the protruding shape around the melting zone, that is, the formation of re-solidified droplets were studied from a fluid perspective [20].

In particular, since the laser beam concentrates high-density energy on a local element, the surface shape changes due to the scribing width and depth due to the difference in height between the screw thread and the bone when surface-treating the screw-type implant and the secondarily generated elevation. When processed arbitrarily without considering these problems, a uniform surface shape cannot be realized, and relief annealing and a surface oxide film cannot be uniformly formed.

It is essential to establish precise and systematic process parameters when performing the surface treatment of implants using lasers. Therefore, this study intends to use a Q-switching Nd:YAG laser with a wavelength of 1.06 μm to develop a process for modifying the surface of an implant so that it can become a biocompatible structure.

2. THEORY

Since Ti, like an implant material, is a good conductor, it has a high conductivity, and the penetration depth of the electric field can be defined as follows [21]:

$$\delta = \frac{1}{\sqrt{\pi f \mu \sigma}} \quad , \tag{1}$$

where μ is the magnetic permeability; σ is the electrical conductivity. In Eq. 1, the penetration depth decreases as the frequency and conductivity increase. In this study, the depth of penetration expressed by Eq. 1 is intended to suggest changes in surface behavior when a laser is irradiated on implant materials.

3. EXPERIMENTAL METHODS

In this study, Ti-6Al-4V alloy, a representative material of α+β alloy, was used as the implant material in Table 1. The irradiation characteristics and process characteristics of the laser beam were tested using pure titanium.

The size of the screw-type implant specimen and the size of the thread and bone of the surface treatment part were, on average, 540 μm and 740 μm, respectively. As a way to irradiate the laser beam on the screw bone, pure titanium, and Ti-6Al-4V specimens were produced for the experiment in order to consider various physical characteristics related to the determination of the spot size of the laser beam and the depth of the hole formed on the surface. The laser beam was experimented with in a single pass, and after setting the non-overlapping range and the overlapping range, a preliminary study was conducted. The laser used in the experiment was a Q-switching Nd:YAG Fiber.

The voltage (I) of Q-switching Nd:YAG was tested by changing the step size (μm), output (Power:%), frequency (kHz), and duty after fixing 16.8 A and Mark Delay (usec).

The laser used in this study was Nd:YAG, and the output is 90 W in the multimode and 18 W in TEM00. The wavelength was 1.06 μm, and the focus size was 60 – 80 μm. Liu have reported a simple technique to diagnose the energy distribution of high-power pulsed-laser beams by direct imaging the contour of specific-threshold energy fluences [22]. FreeMark-10 was used as a scanner to control the transfer speed of the beam. Fig. 1 is a schematic diagram of the implant surface treatment laser system.

Table 1. Chemical composition of implant material, wt.%

	C (max)	N	H	O	Fe	Al	V	Ti
Ti-6Al-4V	0.08	0.05	0.012	0.13	0. 0.25	5.5~6.5	3.5~4.5	Bal
Pure Ti	–	–	–	–	0.067	0.796	0.067	Bal

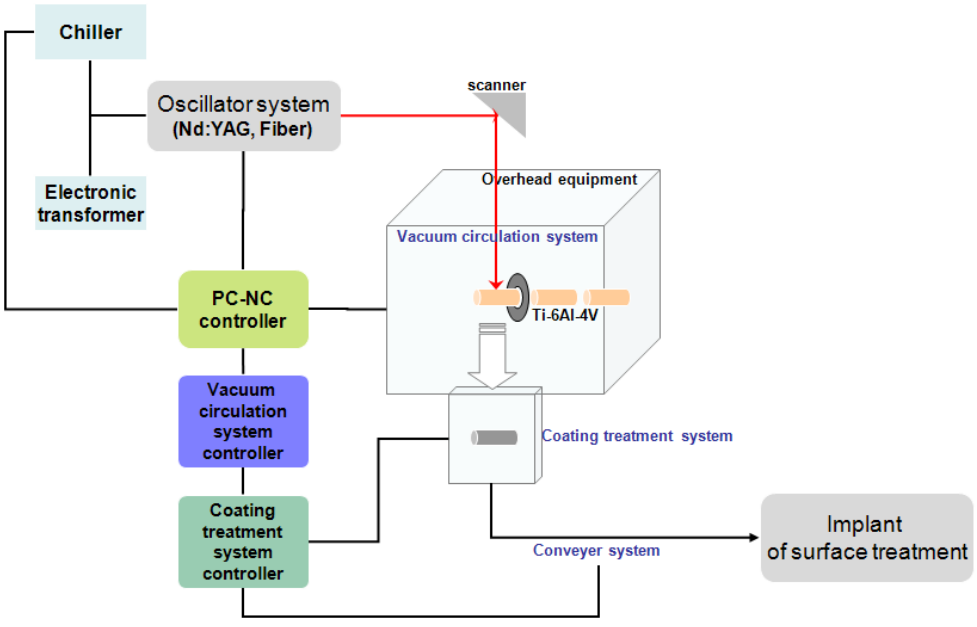

Fig. 1. Schematic diagram of experimental equipment

Since implants are very small in size and have a circular shape, they can be affected by various parameters related to laser process variables, such as the focus position and irradiation angle, during laser surface treatment. In order to control this, we experimented by attaching a micro stage and a rotating axis to control the rotating X, Y, and Z axes. Furthermore, since the implant is circular and has a fine angle along with the screw thread and the screw bone, it is necessary to precisely change the tilting angle. The experimental apparatus was configured to control the tilting angle (0 – 30°: Resolution (0.1°)).

Various control equipment was attached to control the positional accuracy, but in order to confirm the exact position of the laser beam, the position was identified using a monitoring system for the experiment. In this study, a stereo microscope equipped with a CCD camera was used to observe the processing of the Q-switching Nd:YAG laser. This monitoring system is used to correct the irradiation position of the He-Ne laser, which is a guide beam.

In this study, a laser beam was irradiated onto the implant surface using an F-Theta lens as a beam transmission lens to effectively deliver the laser beam to the implant surface. The F-Theta lens can be used very effectively in implant surface treatment because the Gaussian beam is uniformly irradiated and has a fast beam transfer speed.

In order to analyze the material change on the surface when the laser beam is irradiated on the surface of pure titanium thin plate and implant, a 3-dimensional surface roughness meter (Accura 2000, IN-TEK Plus, Korea) and an optical microscope (Olympus: GX-51, Japan) capable of observing the roughness of microregions were used.

4. EXPERIMENTAL RESULTS AND DISCUSSION

The Nd:YAG fiber laser used in this experiment had a wavelength of 1.06 μm. Calculating this as a frequency is $f\lambda = c$, so 2.8×10^{14} Hz. Penetration depth (Eq. 1) was calculated using Ti's conductivity (1.8×10^{6} S/m) and laser frequency (2.8×10^{14} Hz), and magnetic permeability ($4\pi \times 10^{-7}$H/m). The characteristics according to the process variable change for implant surface processing were analyzed using the penetration depth expressed in Eq. 1 as a variable.

Laser processing variables that affect the surface shape include wavelength, energy, pulse time, mode shape, repetition rate, and focus position. Laser energy densities of 4.0 (23.8) and 13.6 J/cm^2 for laser wavelengths of 1064 and 532 nm, respectively, were found to be sufficient for inducing surface modifications of the samples [20].

After irradiating the laser beam, as the irradiated area melts or vaporizes, grooves are dug and stress is applied to the surface of the processing medium. Therefore, the laser process variable was appropriately adjusted for the part that varies depending on the type of laser and the control variable used. The used process variables were voltage, output, overlap, frequency, and duty.

Fig. 2 shows the test result after cutting the Ti-6Al-4V test piece into a longitudinal section, and the surface treatment of the implant was precisely investigated while maintaining the working position and non-focal distance constant on a general flat plate and rotating it.

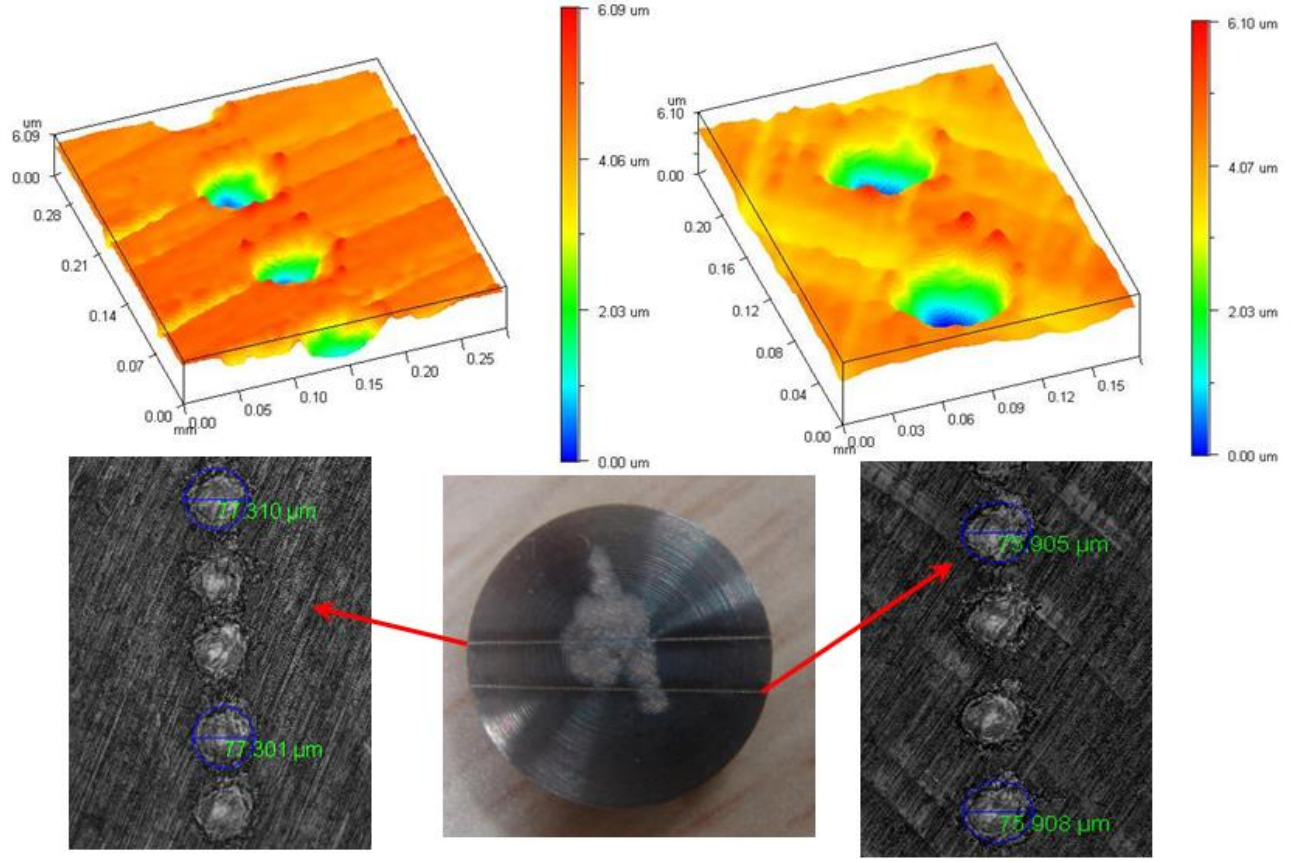

Fig. 2. Test result after the longitudinal section cut

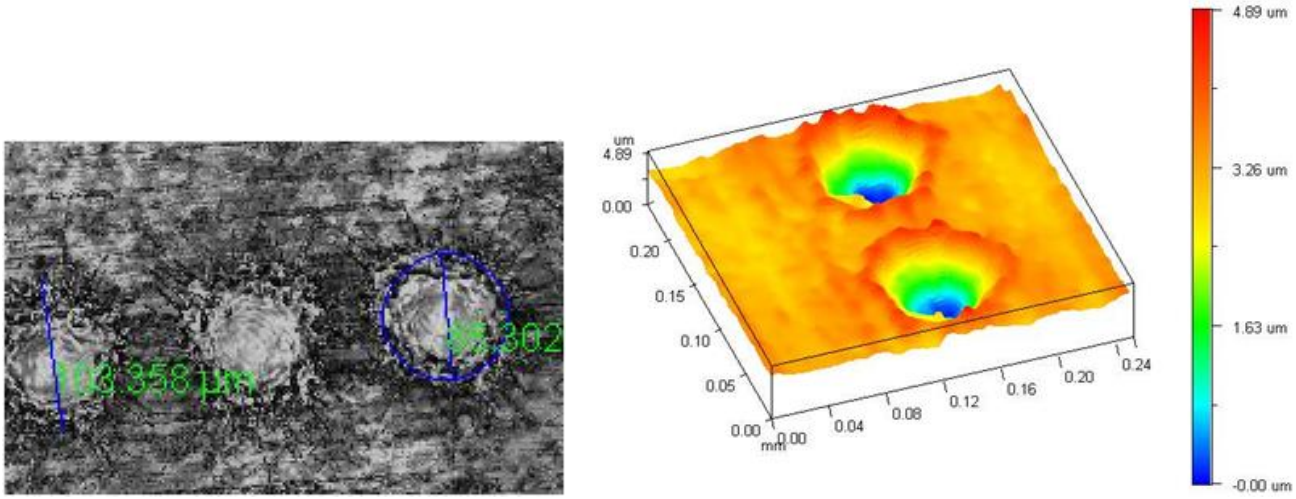

Power, %:100, frequency, kHz:1, duty: 50

Fig. 3. Surface shape according to change of laser overlap (P_{ER}: 0%, width, μm: 85.302)

Fig. 3 shows the processing characteristics according to the change in the laser beam overlap of the pulsed laser. If the scanning speed of the laser beam is *V*, the focal size of the focusing beam is *D*, and the moving distance of the focal size according to the scanning speed is *V*, the degree of overlap P_{ER} in the pulse laser can be expressed as a ratio to the non-overlapping distance S from the origin [11].

$$P_{ER} = \left(1 - \frac{S'}{S}\right) \times 100, \quad (2)$$

where $S' = V \times T_F$ and $S = D + V \times T_P$; T_F is the period between pulses; T_P is the pulse period, that is, the pulse width. When calculating the degree of overlap, the beam diameter was measured while considering the heat-affected zone. In Fig. 3, the beam size is shown on the left, and the measurement result obtained with a surface measuring instrument is shown on the right. Although the surface of the specimen appears to be overlapped due to the effect of the heat-affected zone, the degree of overlap was measured differently in the surface roughness tester. When the experiment was performed while decreasing the degree of overlap, the characteristics of the implanted specimen after irradiating the pulse beam on its surface were clearly identified.

In one attempt [23], the low power laser was applied to create the surface porosity of different magnitude. Examined the osseointegration of laser-textured titanium alloy (Ti6Al4V) implants with pore sizes of 100, 200, and 300 μm.

The scribing width increased as the degree of overlap increased, and when the degree of overlap was 65 %, it was 145.595 μm, and when the degree of overlap was 0 %, the diameter that penetrated into the implant surface was 77.219 μm. As the degree of overlap increased, the heat diffused to the periphery due to the energy accumulated by the laser beam, and the scribing width increased. When the degree of overlap was 0 %, a single pulse was irradiated to the implant surface and absorbed, and then the heat was quickly transferred to the inside and surroundings and condensed, resulting in a relatively small penetration diameter.

Considering the case where the penetration depth calculated by Eq. 1 is 2.2 μm, the number of pulses irradiated is 100 Hz. The penetration was about 38 times greater than the calculated value by a single pulse due to the heat loss caused by different resistances depending on the metal material caused by the alloy composition.

Research on osseointegration primarily focuses on surface modifications of titanium endosseous implants to enhance fusion with bone tissue[24 – 26].

Mukherjee et al. [27] found that the laser ablation induced micro-grooves and ripples on the laser treated Ti-6Al-4V were dependent on the laser scanning parameters and, moreover, influenced the cellular activities and enhanced the biocompatibility. Lawrence et al. [28] indicated that the adhesiveness and proliferation of osteoblast cells can be enhanced when Ti-6Al-4V alloy was treated by a pulsed Nd : YAG laser, owing to the increased surface roughness and improved wettability. This observed increase in the surface roughness following resolidification indicates that the liquid Ti6Al4V alloy flow within the meltpool was turbulent. This accords with the work [20, 27, 28], who have reported that laser wavelengths increase the titanium surface roughness.

Since the area of the implant and the bone density of the patient cannot be changed arbitrarily when implanted in the patient, increasing the effective surface area of the implant becomes a factor contributing to strong adhesion to the patient's dentine. If the surface is ablated with a laser beam to increase the effective surface area of the implant, the increased surface area makes it firmly attached to the dentine. The change in the surface due to the ablation of the surface by the laser beam is shown in Fig. 3 when the degree of overlap is 0 %.

Fig. 4 examines P_{ER}, the change in scribing width according to the power (%) for the same working distance when the frequency and duty are fixed. Within 50 to 100 % of the power of the maximum output of this experimental apparatus, the change in scribing width was only about 10 μm. However, when the power was 80 – 100 %, the scribing depth was larger than in other processes.

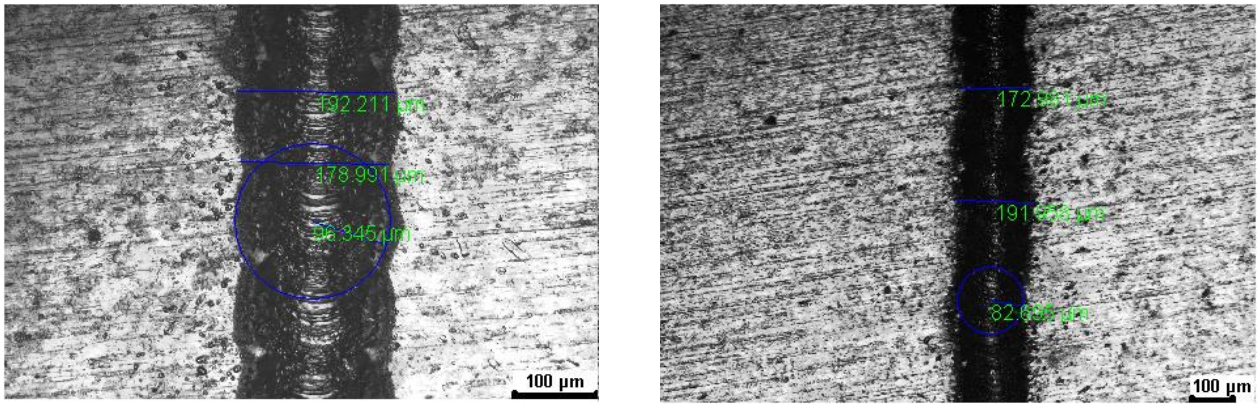

a b

Fig. 4. Scribing width according to change of laser power (P_{ER}: 70%, frequency, kHz: 1, duty: 15): a – power, %: 95, width, μm: 178.991; b – power, %: 85, width, μm: 172.981

It is a phenomenon in which the depth of penetration increases as energy groups per unit of time accumulate on the surface of the implant as the power density increases.

Fig. 5 shows the change in scribing width according to the duty increase. When the time between pulses is T_F and the pulse duration or pulse width is T_P, the variable defined as T_P/T_F becomes the load cycle and duty. The scribing width increased from about 98.436 μm to 153.693 μm until the duty value was 10 to 60, and then when the duty value was further increased to 70 to 80, the scribing width decreased to some extent.

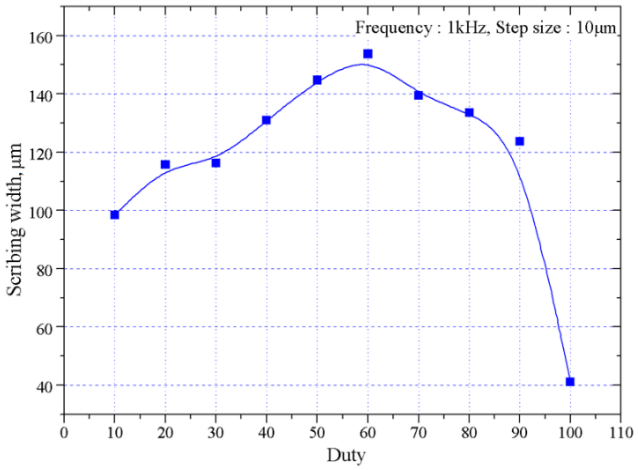

Fig. 5. Change of scribing width after laser beam irradiation

Experimental results showed that the scribing width increased up to a duty cycle of 60 and then decreased as the duty cycle further increased. Since an increase in the duty cycle means an increase in the pulse width, it indicates that the characteristics of the pulse laser are changed to the characteristics of the continuous wave laser.

As a result, as shown in Fig. 3, the laser beam, which should have penetrated the implant surface in a very short time due to ablation, manifested as energy loss due to heat transfer from the surface to the inside. The same result was obtained even when the duty cycle decreased as the period between pulses decreased. The laser used in this study was a 4-level laser, and the pulse should be instantaneously oscillated by sufficient density inversion at the upper level during the pulse period. This phenomenon occurred because the energy density of the upper level was lowered as the duty period was extended to the lower level for a long period of time.

Fig. 6 shows the change in the scribing width according to the change in the kurtosis expressed by Eq. 2. The result of the experiment was shown while changing the degree of overlap with the frequency and duty fixed at 1 kHz and 50, respectively. When the degree of overlap was less than 40 %, the scribing width appeared relatively small. When the beams of the pulsed laser were independently irradiated on the surface of the specimen in the form of single pulses, the degree of overlap was small.

When the overlapping degree increased to 60 % or more, the scribing width increased rapidly. This was a phenomenon that occurred when a pulse laser beam irradiated a specimen to cause melting and increased the irradiation rate by overlapping another pulse beam before heat spread to the periphery.

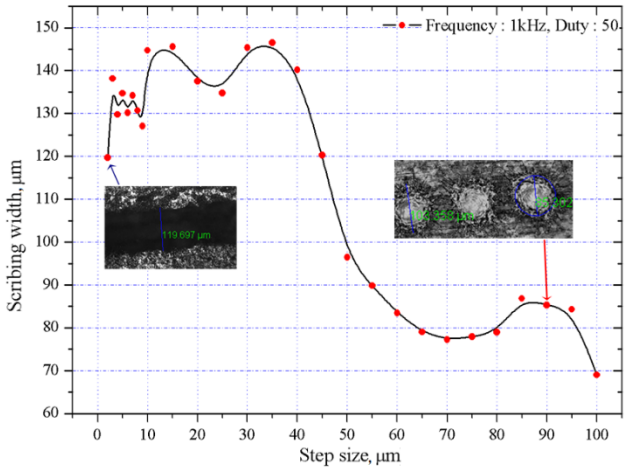

Fig. 6. Scribing width according to change of overlap of overlap

In this experimental condition, when the degree of overlap exceeded 90 %, the scribing width started to temporarily decrease as the amount of evaporation increased. Such a phenomenon was undesirable for surface treatment to increase the cross-sectional area of the implant surface. When the degree of overlap was greater than 90 % and evaporation and melting occurred rapidly, it did not meet the purpose of increasing the contact area with the

tooth bone. This phenomenon may lead to a reduction in the diameter of the implant due to the evaporation of the material from the surface, causing problems with its strength and resulting in very undesirable results.

5. CONCLUSIONS

The following conclusions were obtained by examining the surface behavior when the laser was irradiated on the implant material using the Nd:YAG laser.

1. Since the bonding between bone and implant is a very important factor, it is essential to treat the implant's surface into an efficient and stable geometric shape.
2. When the power was 80 – 100 %, the scribing depth was larger than in other processes. As the power density increased, the penetration depth increased as the energy accumulated per unit of time on the implant surface.
3. The scribing width increased up to the duty cycle of 60, and then decreased as the duty cycle further increased.
4. When the overlapping degree increased to 60 % or more, the scribing width increased rapidly. When the overlapping degree exceeded 90 %, the evaporation amount increased and the scribing width started to temporarily decrease.
5. The results of this study suggest that implant surface treatment technology using lasers will be secured and used for actual implant surface treatment
6. Although biological experiments have not been conducted, future clinical trials (in vitro) may improve implant osseointegration.

REFERENCES

1. **Zhu, G., Wang, J., Li, J.J.** Advances in Implant Surface Modifications to Improve Osseointegration *Materials Advances* 21 2021: pp. 6901 – 6927. https://doi.org/10.1039/d1ma00675d
2. **Donatella, D., Federico, M., Maria, G.F.** Biomaterials for Dental Implants: Current and Future Trends *Journal of Materials Science* 50 2015: pp. 4479 – 4812. https://doi.org/10.1007/s10853-015-9056-3
3. **Niinomi, M.** Metallic Biomaterials *Journal of Artificial Organs* 11 2008: pp. 105 – 110. https://doi.org/10.1007/s10047-008-0422-7
4. **Bo˙zena, Ł., Patrycja, O., Delfina, N., Joanna, M.** Developments in Dental Implant Surface Modification *Coatings* 15 (1) 2025: pp. 109 – 145. https://doi.org/10.3390/coatings15010109
5. **Bo˙zena, Ł., Julian, K., Patrycja, O., Maciej, Z.** EIS and LEIS Study on In Vitro Corrosion Resistance of Anodic Oxide Nanotubes on Ti–13Zr–13Nb Alloy in Saline Solution *Coatings* 13 (5) 2023: pp. 875 – 893. https://doi.org/10.3390/coatings13050875
6. **SmoŁka, A., Rodak, K., Dercza, G., Dudek, K., Łosiewicz, F.B.** Electrochemical Formation of Self-Organized Nanotubular Oxide Layers on Ti13Zr13Nb Alloy for Biomedical Applications *Acta Physica Polonica A* 125 (4) 2014: pp. 932 – 935. https://doi.org/10.12693/APhysPolA.125.932
7. **Rajaeirad, M., Fakharifar, A., Posti, M.H.Z., Khorsandi, M., Watts, D.C., Elraggal, A., Ouldyerou, A., Merdji, A., Roy, S.** Evaluating the Effect of Functionally Graded Materials on Bone Remodeling Around Dental Implants *Dental Materials* 40 2024: pp. 858 – 868. https://doi.org/10.1016/j.dental.2024.04.002
8. **Dommeti, V.K., Roy, S., Pramanik, S., Merdji, A., Ouldyerou, A., Özcan, M.** Design and Development of Tantalum and Strontium Ion Doped Hydroxyapatite Composite Coating on Titanium Substrate: Structural and Human Osteoblast-Like Cell Viability Studies *Materials* 16 (4) 2023: pp. 1499 – 1517. https://doi.org/10.3390/ma16041499
9. **Ouldyerou, A., Mehboob, H., Merdji, A., Aminallah, L., Mehboob, A., Mukdadi, O.M.** Biomechanical Analysis of Printable Functionally Graded Material (FGM) Dental Implants for Different Bone Densities *Computers in Biology and Medicine* 150 2022: pp. 106111. https://doi.org/10.1016/j.compbiomed.2022.106111
10. **Ouldyerou, A., Merdji, A., Aminallah, L., Roy, S., Mehboob, H., Özcan, M.** Biomechanical Performance of Ti-PEEK Dental Implants in Bone: An in-Silico Analysis *Journal of the Mechanical Behavior of Biomedical Materials* 134 2022: pp. 105422. https://doi.org/10.1016/j.jmbbm.2022.105422
11. **Kim, J.W., You, Y.T.** Fiber Laser Welding Properties of Copper Materials for Secondary Batteries *Materials Science (Medžiagotyra)* 23 (4) 2017: pp. 398 – 1403. https://doi.org/10.5755/j01.ms.23.4.16316
12. **Gaggl, A., Schultes, G., Muller, W.D., Karcher, H.** Scanning Electron Microscopical Analysis of Laser-Treated Titanium Implant Surfaces a Comparative Study *Biomaterials* 21 (10) 2000: pp. 1067 – 1073. https://doi.org/10.1016/S0142-9612(00)00002-8
13. **Peto, G., Karacs, A., Paszti, Z., Guczi, L., Divinyi, T., Joob, A.** Surface Treatment of Screw Shaped Titanium Dental Implants by High Intensity Laser *Applied Surface Science* 186 (1 – 4) 2002: pp. 7 – 13. https://doi.org/10.1016/S0169-4332(01)00769-3
14. **Karacs, A., Fancsaly, A.J., Divinyi, T., Peto, G., Kovach, G.** Morphological and Animal Study of Titanium Dental Implant Surface Induced by Blasting and High Intensity Pulsed Nd-glass Laser *Materials Science and Engineering: C* 23 (3) 2003: pp. 431 – 435. https://doi.org/10.1016/S0928-4931(02)00316-8
15. **Cho, S.A., Pakr, K.T.** The Removal Torque of the Laser-Treated Titanium Implants in Rabbit Tibia Treated by Dual Acid Etching *Biomaterials* 24 (20) 2003: pp. 4859 – 4863. https://doi.org/10.1016/S0142-9612(03)00218-7
16. **Yue, T.M., Cheung, T.M., Man, H.C.** The Effects of Laser Surface Treatment on the Corrosion Properties of Ti-6Al-4V Alloy in Hank`s Solution *Journal Materials Science Letters* 19 2000: pp. 205 – 208. https://doi.org/10.1023/A:1006750422831
17. **Yue, T.M., Yu, J.K., Mei, Z., Man, H.C.** Excimer Laser Surface Treatment of Ti-6Al-4V Alloy for Corrosion Resistance Enhancement *Materials Letters* 52 2002: pp. 206 – 212. https://doi.org/10.1016/S0167-577X(01)00395-0
18. **Guillemot, F., Prima, E., Tokarev, V.N., Belin, C., Porté-Durrieu, M.C., Gloriant, T., Baquey, Ch., Lazare, S.** Ultraviolet Laser Surface Treatment for Biomedical Applications of Titanium Alloys: Morphological and Structural Characterization *Applied Physics A* 77 2003: pp. 899 – 904. https://doi.org/10.1007/s00339-003-2162-0
19. **Bereznai, M., Pelsoczi, I., Toth, Z., Turzo, K., Radnai, M., Bor, Z., Fazekas, A.** Surface Modifications Induced by ns and sub-ps Excimer Laser Pulses on Titanium Implant Material *Biomaterials* 24 2003: pp. 4197 – 4203.

https://doi.org/10.1016/S0142-9612(03)00318-1

20. **Trtica, M., Gakovic, B., Batani, D., Desai, T., Panjan, P., Radak, B.** Surface Modifications of a Titanium Implant by a Picosecond Nd:YAG Laser Operating at 1064 and 532 nm *Applied Surface Science* 253 (23) 2006: pp. 2551 – 2556. https://doi.org/10.1016/j.apsusc.2006.05.024
21. **Götz, H.E., Müller, M., Emmel, A., Holzwarth, U., Erben, R.G., Stangl, R.** Effect of Surface Finish on the Osseointegration of Laser-treated Titanium Alloy Implants *Biomaterials* 25 (18) 2004: pp. 4057 – 4864. https://doi.org/10.1016/j.biomaterials.2003.11.002
22. **Liu, J.M.** Simple Technique for Measurements of Pulsed Gaussian-beam Spot Sizes *Optics Letters* 7 (5) 1982: pp. 196 – 198. https://doi.org/10.1016/j.jobe.2022.104393
23. **Chung, D.D.L., Ozturk, M** Electromagnetic Skin Depth of Cement Paste and its Thickness Dependence *Journal of Building Engineering* 52 (15) 2022: pp. 104393. https://doi.org/10.1016/j.jobe.2022.104393
24. **Le Guehennec, L., Soueidan, A., Layeolle, P., Amourinq, H.E.** Surface Treatments of Titanium Dental Implants for Rapid *Dental Materials* 23 2007: pp. 844 – 854. https://doi.org/10.1016/j.dental.2006.06.025
25. **Lee, U.L., Yun, S., Lee, H., Cao, H.L., Woo, S.H., Jeong, Y.H., Jung, T.G., Kim, C.M., Choung, P.H.** Osseointegration of 3D-printed Titanium Implants with Surface and Structure Modifications *Dental Materials* 38 2022: pp. 1648 – 1660. https://doi.org/10.1016/j.dental.2022.08.003
26. **Kurup, A., Dhatrak, P., Khasnis, N.** Surface Modification Techniques of Titanium and Titanium Alloys for Biomedical Dental Applications: A Review *Materials Today: Proceedings* 39 (18) 2021: pp. 84 – 90. https://doi.org/10.1016/j.matpr.2020.06.163
27. **Mukherjee, S., Dhara, S.** Enhancing the Biocompatibility of Ti6Al4V Implants by Laser Surface Microtexturing: an in Vitro Study *The International Journal of Advanced Manufacturing Technology* 76 2015: pp. 5 – 15. https://doi.org/10.1007/s00170-013-5277-2
28. **Lawrence, J., Hao, L., Chew, H.R.** On the Correlation between Nd:YAG Laser-induced Wettability Characteristics Modification and Osteoblast Cell Bioactivity on a Titanium Alloy *Surface and Coatings* 200 2006: pp. 5581 – 5589. https://doi.org/10.1016/j.surfcoat.2005.07.